UC Irvine
UC Irvine Previously Published Works

Title
Fractional snow cover in the Colorado and Rio Grande basins, 1995-2002

Permalink
https://escholarship.org/uc/item/2707659f

Journal
Water Resources Research, 44(1)

ISSN
00431397

Authors
Bales, R. C
Dressler, K. A
Imam, B.
et al.

Publication Date
2008

DOI
10.1029/2006WR005377

Peer reviewed

Fractional snow cover in the Colorado and Rio Grande basins, 1995–2002

R. C. Bales,[1] K. A. Dressler,[2] B. Imam,[3] S. R. Fassnacht,[4] and D. Lampkin[5]

[1] A cloud-masked fractional snow-covered area (SCA) product gridded at 1 km was developed from the advanced very high resolution radiometer for the Colorado River and upper Rio Grande basins for 1995–2002. Cloud cover limited SCA retrievals on any given 1-km^2 pixel to on average once per week. There were sufficient cloud-free scenes to map SCA over at least part of the basins up to 21 days per month, with 3 months having only two scenes sufficiently cloud free to process. In the upper Colorado and upper Grande, SCA peaked in February–March. Maxima were 1–2 months earlier in the lower Colorado. Averaged over a month, as much as 32% of the upper Colorado and 5.5% of the lower Colorado were snow covered. Snow cover persisted longest at higher elevations for both wet and dry years. Interannual variability in snow cover persistence reflected wet-dry year differences. Compared with an operational (binary) SCA product produced by the National Operational Hydrologic Remote Sensing Center, the current products classify a lower fraction of pixels as having detectable snow and being cloud covered (5.5% for SCA and 6% for cloud), with greatest differences in January and June in complex, forested terrain. This satellite-derived subpixel determination of snow cover provides the potential for enhanced hydrologic forecast abilities in areas of complex, snow-dominated terrain. As an example, we merged the SCA product with interpolated ground-based snow water equivalent (SWE) to develop a SWE time series. This interpolated, masked SWE peaked in April, after SCA peaked and after some of the lower-elevation snow cover had melted.

1. Introduction

[2] Seasonal snow cover in the mountains of the western U.S. accumulates much of the water that becomes streamflow, fills water supply reservoirs and recharges critical groundwater aquifers in the spring and summer months. In the semiarid Southwest, snow cover patterns influence summer soil moisture and subsequent monsoon activity [*Gutzler and Preston*, 1997]. Therefore snow-covered area (SCA) is an important hydrologic variable for streamflow prediction [*Rango and Martinec*, 1979] and observations of areal extent have been used in some hydrologic forecasts for decades [*Maurer et al.*, 2003]. Nevertheless, estimating snow cover properties at a basin scale, particularly snow water equivalent (SWE) but also SCA, remains a challenge.

[3] Routine satellite monitoring of snow extent in the United States began in 1966 with weekly monitoring of snowpack using NOAA's advanced very high resolution radiometer (AVHRR) satellite. Further understanding of the radiative properties of snow in the 1970s [*Dozier et al.*, 1981] resulted in more accurate SCA mapping, and set the stage for greater use of SCA products in hydrology in the 1980s [e.g., *Martinec et al.*, 1991]. As an operational satellite with daily temporal resolution and large spatial coverage, AVHRR is well suited for routine use in water resources. Although binary SCA products have been available for some years (http://www.nohrsc.nws.gov/), they have not found wide use in operational hydrologic forecasting owing to concerns about accuracy and the lack of operational models that could benefit from SCA data. Various research investigations have shown the potential for accurate mapping of snow cover from cloud-free AVHRR scenes [e.g., *Metsämäki et al.*, 2002, 2005; *Foppa et al.*, 2004].

[4] With only five bands, AVHRR/2 offers less potential for accurate discrimination of clouds and various land cover classes as compared to Landsat or Moderate Resolution Imaging Spectroradiometer (MODIS) [*Dozier*, 1989]. How-

---

[1] School of Engineering, University of California, Merced, California, USA.

[2] Penn State Institutes of Energy and the Environment, Pennsylvania State University, University Park, Pennsylvania, USA.

[3] Department of Civil and Environmental Engineering, Henry Samueli School of Engineering, University of California, Irvine, California, USA.

[4] Watershed Science Program, Colorado State University, Fort Collins, Colorado, USA.

[5] Department of Geography, Pennsylvania State University, University Park, Pennsylvania, USA.
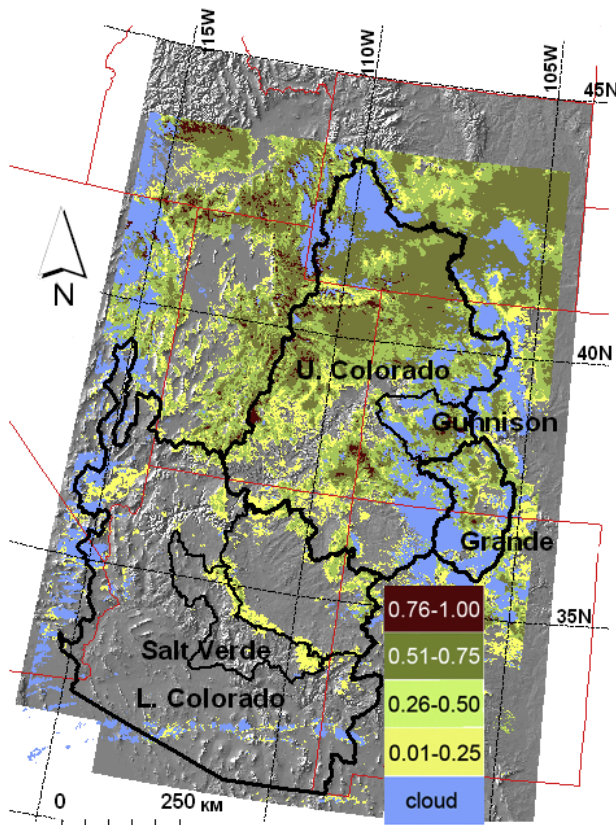
Figure 1. Area mapped, showing state and watershed boundaries, along with sample result for 7 February 1997 showing fraction SCA binned into four values plus clouds. Outlines are shown for the upper and lower Colorado River, Salt-Verde River, Gunnison River, and Rio Grande basins. Area not shaded was snow free.

ever, Landsat has a 14-day repeat cycle, which limits its suitability for operational snow products. Although MODIS provides daily coverage, it is a research, not operational satellite. It should be noted that the AVHRR/3 sensor, first carried on NOAA 15, has a sixth channel (channel 3A, 1.6 μm), which provides improved snow/cloud discrimination as compared to AVHRR/2 (up through NOAA 14).

[5] Discrimination of snow and cloud from clear land is somewhat uncertain, particularly because of low-illumination conditions, dense forest masking of snow on the ground, and similarities in the snow/cloud signature in mountains region [*Simpson et al.*, 1998]. Nevertheless, the recent extension of algorithms for fractional SCA mapping [*Rosenthal and Dozier*, 1996] to AVHRR opens up the possibility for more product development, evaluation and use.

[6] The broader objective of the work reported here was to develop a history of snow cover for the Colorado River and Rio Grande basins in the Southwestern U.S., and to advance the use of these satellite snow products in hydrologic science and applications. The principal aims of the analysis reported in this paper were to evaluate the spatial patterns of snow cover persistence over the period 1995–2002 for these areas, to evaluate spatial characteristics of a

product blending satellite SCA with ground-based SWE, and to introduce the SCA data set to a broader community.

2. Study Area

[7] We defined a rectangular analysis area in Albers equal area projection (X: −1873160 to −682160, Y: 904025 to 2458025) that included both the Colorado and upper Grande basins (Figure 1). The upper Colorado River basin is somewhat smaller and higher elevation than is the lower Colorado, though both have comparable fractions of forest cover (Table 1). Note that almost 60% of the upper Colorado, but only 16% of the lower Colorado is above 2,000 m elevation. The snow in the lower basin is located along the Mogollan Rim in eastern central Arizona, up through the Colorado Plateau approaching the Grand Canyon, and in western New Mexico. The upper Rio Grande and two comparable Colorado River subbasins, the Gunnison River basin in the upper Colorado, and the Salt-Verde in the lower Colorado, were selected for further analysis.

3. Methods and Data

[8] Snow-covered area maps for the Rio Grande and Colorado River basins were developed for an 8-year period (1995–2002) from AVHRR scenes using a three-part cloud masking procedure and spectral unmixing algorithm. Using this approach fractional SCA in each pixel was estimated and gridded to 1 km^2. Since some clouds were present in most scenes, all scenes with at least one major headwater basin cloud free were processed. Level 1b AVHRR scenes (NOAA 12 and NOAA 14) were acquired through both the University of California, Santa Barbara, and New Mexico State University. Both sites use the TeraScan system (Sea-Space Corporation) to navigate AVHRR data. Processing occurred in three steps, following the procedure described previously by *Davis et al.* [1999]. First, images were converted from digital counts to radiances for all 5 bands, then to surface reflectance for bands 1 (0.58–0.68 μm), 2 (0.725–1.10 μm), and 3 (3.55–3.93 μm), and to brightness temperature for bands 3 (3.55–3.93 μm), 4 (10.3–11.3 μm), and 5 (11.5–12.5 μm). Atmospheric corrections were made on the reflectance bands (1–3) [*Vermote et al.*, 1997]. These three bands were then introduced into a decision tree algorithm, which is based on training against a set of 532 cases of mixtures of 23 theoretical spectra of snow, vegetation, and snow types [*Rosenthal and Dozier*, 1996]. The

Table 1. Characteristics of Watersheds and Subwatersheds

Basin	Area,[a] km^2	Elevation Range,[a] m	Mean Elevation,[a] m	Percent Above 2000 m	Percent Forested[b]
Upper Colorado	277,000	975–4,260	2,150	60	34
Lower Colorado	346,000	0–3,771	1,310	16	25
Grande	36,000	1,700–3,950	2,640	96	12
Gunnison	20,500	1,401–4,229	2,660	84	9
Salt-Verde	35,100	300–3,384	1,550	19	9

[a]Area and elevation are based on 1-km DEM.
[b]Percentage is based on USGS National Landcover Data set.

Table 2. Description of Steps Involved in Cloud Mask

Spectral Test	Description	Features
VNIR/MIR band difference	band 3 to band 4	Detection of cirrus and low-altitude clouds [Phulpin et al., 1989]
TIR band difference	band 4 to band 5	Detection of semi-transparent clouds [Wen and Rose, 1994]
Simpson's test	band 4/band 3	Detection of clouds over snow [Simpson and Keller, 1995]
Single band test threshold	band 2 or band 4	Detection of large cloud features [Saunders and Kriebel, 1988]

decision tree algorithm returned fractional SCA for each pixel likely to be covered by snow, in 15 discrete increments: 0.1, 0.18, 0.21, 0.3, 0.32, 0.38, 0.45, 0.47, 0.56, 0.58, 0.66, 0.74, 0.82, 0.89, and 0.99. The result is a mixed product of snow, clouds, and highly reflective surfaces, which was then corrected to give just the snow cover fraction per pixel.

[9] Second, a supervised cloud mask from four unique techniques (Table 2), chosen for their combined ability to identify clouds of varying radiative properties, was constructed. An additional aperiodic "no data" mask was generated to account for pixels within the study area, but outside the AVHRR swath during overpass.

[10] Third, a temperature mask was generated to eliminate highly reflective surface features that are unlikely to be snow. Many highly reflective surfaces (light colored desert sand, dry lake beds, water) are unlikely to be the same temperature as SCA. Pixels were identified using a supervised classification of brightness temperatures for band 4. Areas with known and consistent highly reflective properties for the study region, such as White Sands, the Great Basin, and Gulf of California, were also reclassified. We interactively georegistered and orthorectified the imagery using a variety of reference images including vector-based hydrography, digital elevation models and previously registered images.

[11] Spatially distributed SWE was estimated daily at a 1-km^2 resolution for the same area for 1990–2002 (1990–1994 data not shown) by interpolating point SWE measurements from 240 ground-based sensors (snow pillows) operated by the U.S. Natural Resource Conservation Service (SNOwpack TELemetry, SNOTEL), followed by masking with the SCA scenes [Fassnacht et al., 2003]. That is, spatially distributed SWE was obtained by masking (multiplying) the interpolated SWE product with the fractional SCA product on a pixel-by-pixel basis. In this way the interpolated SWE maps were adjusted on a pixel-by-pixel basis for the fraction of area determined as snow covered.

[12] As described by Fassnacht et al. [2003], for each grid cell in the basin, all SNOTEL sites within a 200-km radius, including those outside of the basin, were identified. A linear regression was computed between elevation and SWE for all of the SNOTEL sites within the search radius. This hypsometric relationship was used to estimate SWE for each grid cell using a 1-km digital elevation model. A residual was obtained at each grid block where an observing SNOTEL station was located by removing the observed

value from the analysis (i.e., jackknifing) and subtracting the observed SWE from the computed SWE.

[13] Elevation-dependent bias in the residuals was removed by regressing residuals to a datum of 5000 m above sea level using the dry adiabatic lapse rate. Using the same lapse rate for the temperature-based SWE regression as for temperature made it possible to use the same algorithm for both. Once regressed to the common datum, the lapsed residuals were spatially distributed using inverse distance weighting with a power of 2. The gridded residual surface was regressed back to the basin surface using the same lapse rate and subtracted from the hypsometrically derived SWE grid in order to derive the interpolated SWE surface. Daly et al. [2000] used the same approach, except one hypsometric relationship was computed for each subbasin instead of using a moving search radius to compute the hypsometric relationship at each pixel.

[14] It should be noted that the SCA product shows much more spatial variability than does the SWE product, since SCA involves a pixel-by-pixel analysis, whereas SWE before masking is an interpolation of 240 point values over some 650,000 1-km^2 pixels. The interpolated SWE product before masking is not an estimator of pixel-scale or basin-scale SWE, because we do not explicitly account for snow-free areas in the interpolation. That is the purpose of the masking.

4. Results

[15] A sample from 7 February 1997, in which SCA is overlain onto a shaded relief map for the area (Figure 1), illustrates the main features of the SCA product. Clouds are blue and SCA is binned into four ranges. In most scenes there were greater cloud and snow coverages in the upper Colorado and Grande than in the lower Colorado. There were sufficient cloud-free scenes to map snow cover over at least part of the image up to 21 days per month, with 3 months having only two scenes sufficiently cloud free to process (Table 3). Owing to the early morning AVHRR overpass, illumination was an issue in some January and February scenes; this, together with cloud cover issues, meant that in some months no scenes were available.

[16] Because of the large area covered, very few scenes were completely cloud free. Of those scenes mapped, over half of the area was cloud covered (Figure 2). Note especially the upper Colorado basin in 1996–1997, when even scenes that had nearly complete cloud cover were mapped for snow. Those with highest cloud cover provided

Table 3. Number of AVHRR Scenes Processed for SCA Each Month

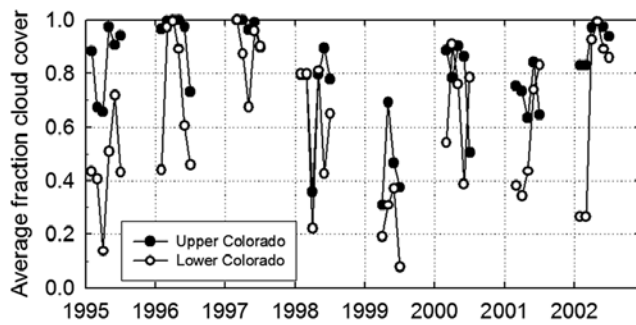|	Jan	Feb	Mar	Apr	May	Jun	Mean
1995	4	7	4	7	4	13	7
1996	10	12	10	16	12	9	12
1997	0	14	21	10	8	8	12
1998	3	2	5	5	4	0	4
1999	0	0	4	5	5	5	5
2000	0	6	6	5	2	7	5
2001	0	3	4	5	8	9	6
2002	2	8	9	8	5	0	5
mean	5	7	10	10	6	8	7

Figure 2. Monthly average fraction cloud cover in scenes mapped. See Table 3 for number of scenes mapped per month.

only subbasin snow cover information. In 1998–1999 fewer scenes were mapped for SCA; that is, those with very limited cloud-free areas were not mapped, and the cloud cover of those scenes was thus lower. However, in 2000–2002 a small number of scenes were mapped, and they had a large fraction of cloud cover. Cloud cover was more frequent in the upper Colorado relative to the lower Colorado basin in 1995–1996, less frequent in 1999 and about the same in other years. The fractions of cloud cover in the upper Grande basin was similar to that for the upper Colorado basin (data not shown). Because of partial cloud

cover the number of scenes per month providing snow cover information on any given pixel was often lower than noted in Table 3. For example, in March 2000 six scenes mapped, but the considerable cloud cover on those days resulted in as few as 2 cloud-free scenes for some high-elevation pixels that month (Figure 3). Clouds were generally more frequent at higher elevations. On average we were able to retrieve SCA for each basin from about one scene per week.

[17] To facilitate intra-annual and interannual comparisons, monthly average SCA was calculated on the basis of an average of all scenes processed during a given month for each year. In both daily and monthly average scenes pixels with any snow cover were dominated by the ≤50% SCA categories (Figure 4).

[18] Maximum basin-wide SCA occurred early in the accumulation period (January–March) and decreased through June. Up to 32% of the upper Colorado (1995), 29% of the upper Rio Grande (1997) and 5.5% of the lower Colorado (1995) were snow covered (Figure 5). Much of the snow in the lower Colorado is located in the Salt-Verde, which was 8.2% snow covered in January 1995. Upper Rio Grande snow cover and depletion patterns generally followed that of the upper Colorado. The year with greatest snow cover was 1995, while the lowest was 1999 in both the upper and lower Colorado. That the latter four years represent a drought period is evident from the trends on Figure 5.
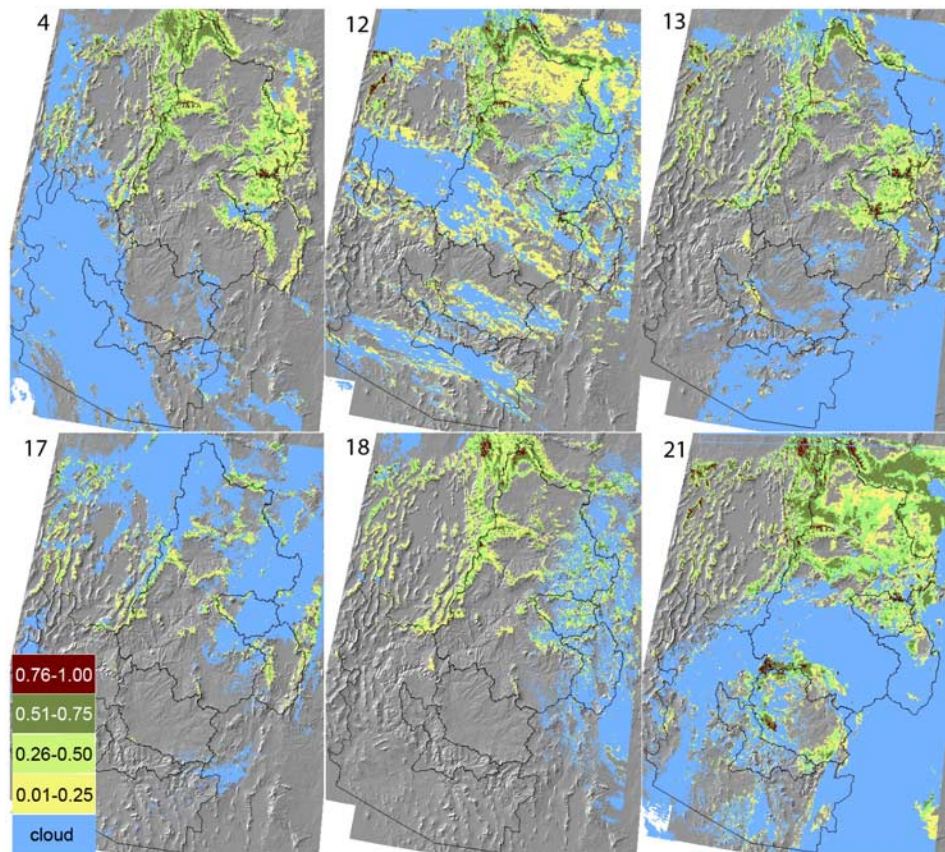

Figure 3. Average fractional snow-covered area, binned into four categories, and cloud cover for scenes mapped in March 2000. Area not shaded was snow free. Dates are indicated in the top left corner of each plot.
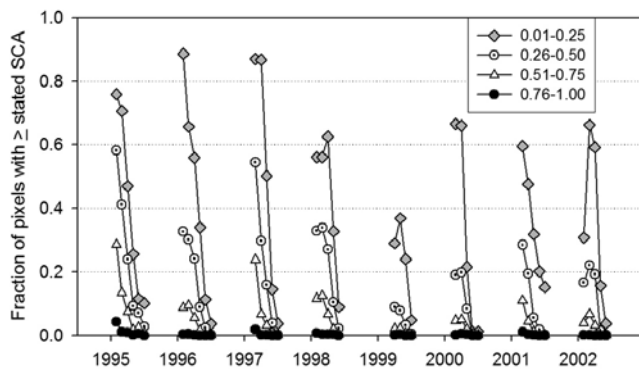
Figure 4. Contribution of different fractional snow cover classes to monthly average total basin snow cover for upper Colorado River basin. For months reported, see Table 3.

[19] The greatest SCA fractions (>25%) occur in high-elevation areas and along basin boundaries (Figures 6 and 7), for both drought and wetter years. In 1995, a relatively wet year, the Gunnison, which is in the upper Colorado, 69% of the pixels had >25% SCA in March, versus only 13% in March 1999, a relatively dry year. In the upper Rio Grande, snow cover is located mostly along the mountainous western and northern portion and to a lesser extent in the mountains forming the eastern boundary. Ablation occurs first at low-elevation areas along the north–south

center of the basins, continuing until June during which snow cover remains in the highest-elevation areas on north and east aspects (Figure 7). A larger percentage of high SCA (>25% per pixel) occurs during wet years (e.g., 1995) as opposed to dry years (e.g., 2000). Similar to the upper Colorado (Figure 4), about 70% of the upper Grande basin's pixels had some snow cover in 1995, versus 60% in February 2000, but the fraction of pixels with SCA >25% in 2000 was about 1/3 that in 1995. Also snow cover depleted much faster in 2000, reflecting less total accumulation. The relative April values for the upper Grande were ~10% SCA in 1995 versus 5% in 2000 (Figure 5c).

[20] Areas with persistent snow cover in March and April for 7–8 of the 8 years studied are limited to the higher elevations of the upper Colorado and Grande basins (Figure 8). Expanding on this, essentially all of the pixels in the upper Rio Grande basin had some snow in the February–March accumulation period for the years mapped (Figure 9). Considering the monthly averages, over 50% accumulated some snow in at least 5 years and 25% had some snow in at least 7 years of the 8 years mapped. Interannual persistence was much weaker during snowmelt (May, Figure 9).

[21] Maximum average SWE occurred in March to April in the upper Rio Grande and generally somewhat earlier in the Salt-Verde (Figure 10); however, in 1997 and 1999 the maximum SWE in the Salt-Verde occurred in April. In the upper Grande the greatest SWE generally coincided spatially with high SCA (>25%) (Figure 11). In 1995 SWE increased from January to a March peak, when 40% of the basin contained >100 mm SWE.
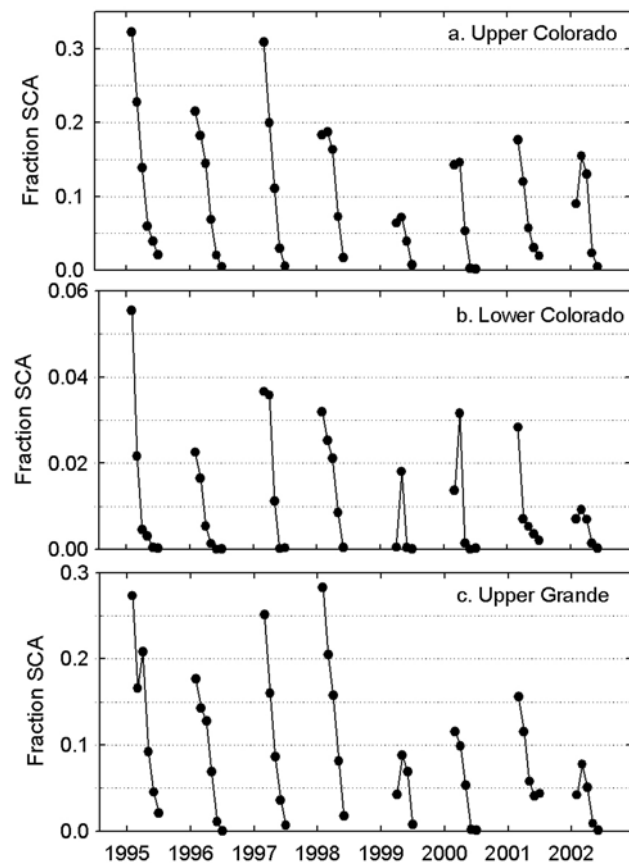
5. Discussion

[22] Topography is a primary control on snow processes and snow characteristics (e.g., density and depth) [*Elder and Dozier*, 1990; *Elder et al.*, 1991; *Blöschl et al.*, 1991], as is evident in snow cover patterns. The current fractional SCA time series indicates that the magnitude of snow coverage changes annually but the general geographic location of snow is repeatable from year to year for both wet and dry years. Interannual variability in snow cover
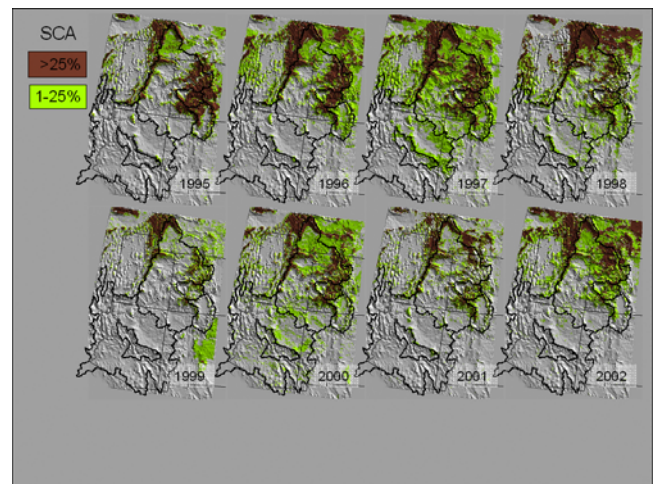

Figure 5. Basin-average SCA for upper Colorado, lower Colorado, and upper Grande basins (monthly averages).

Figure 6. Monthly average SCA for March, with SCA classified as 1–25% or ≥25% SCA.
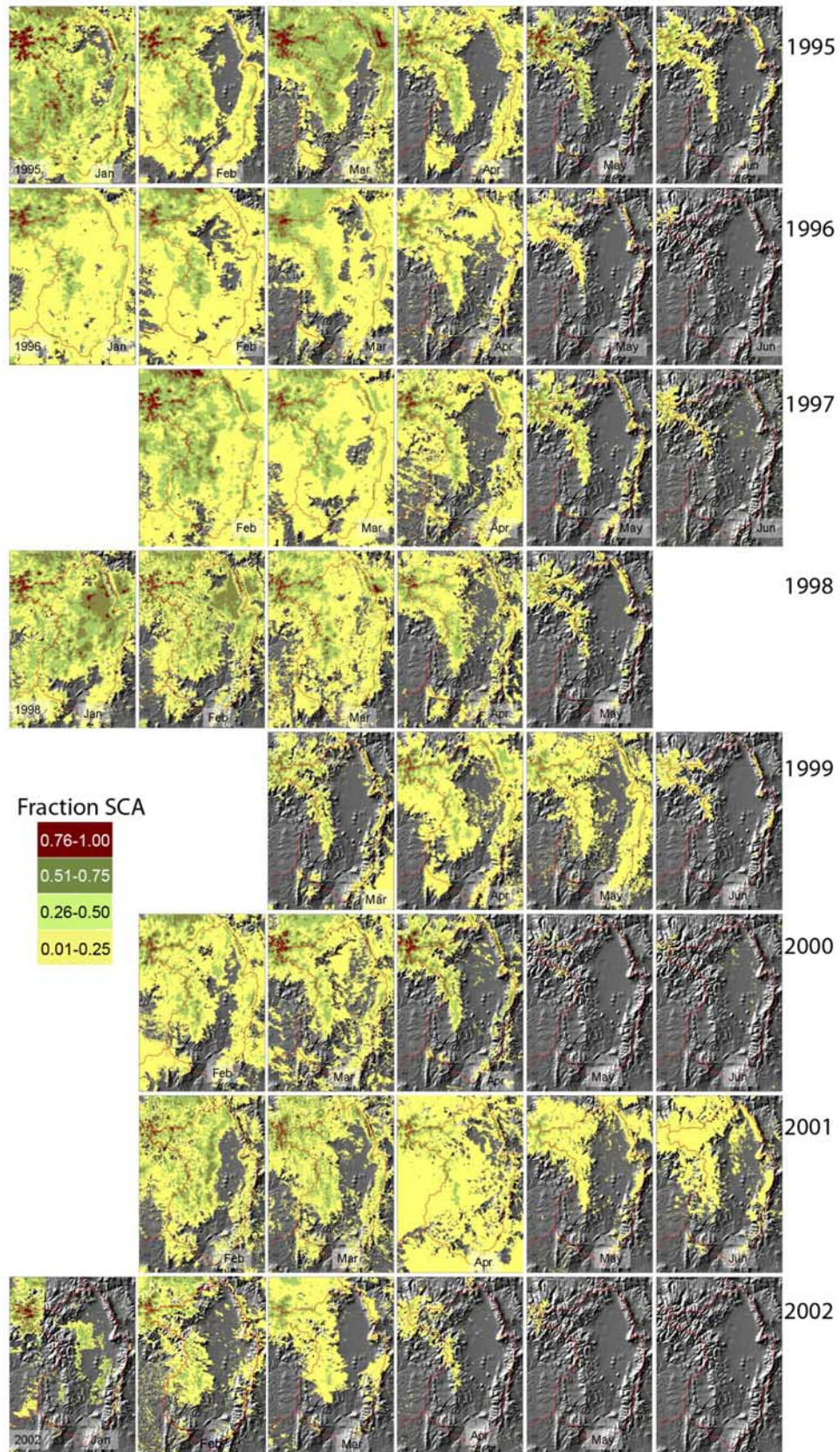
Figure 7. Monthly average SCA for upper Grande basin. Some months were not processed owing to missing data because of, e.g., low illumination (January) and/or cloud cover (February). Area not shaded was snow free.
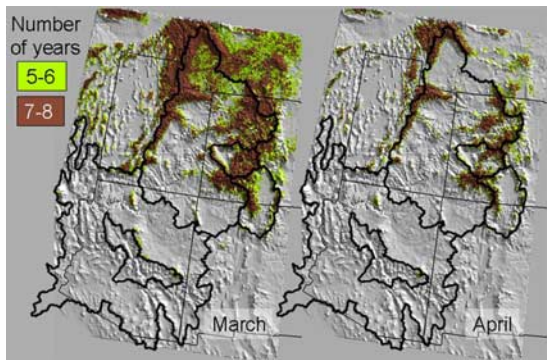
BALES ET AL.: FRACTIONAL SNOW COVER

Figure 8. Snow cover persistence over the 1995–2002 period for March and April, reported as number of years each pixel had detectable snow cover during that month.

persistence does, however, reflect climatic patterns. For 1995–1998 conditions were relatively "wet," i.e., average or above snow accumulation. Following the 1998 El Niño year, 1999–2002 were relatively dry, or drought, conditions, across the western United Stated (cf. U.S. Drought Monitor). Physiographic factors affect snow cover persistence both seasonally and interannually. For example, in the upper Rio Grande, snow cover in wet years (1995–1998) is 15–50% greater on south facing than on north facing slopes in the accumulation period; however as the melt season progresses the fraction SCA on south facing slopes diminishes to about 20–30% less than on north facing slopes by 1 May, and to less than half that on north facing slopes by mid-June (Figure 12). This pattern of south facing slopes accumulating more snow but melting out sooner was not apparent in dry years (1999–2002).

[23] There are significant differences between the current fractional SCA product and the binary SCA product produced routinely from AVHRR by the National Weather Service's National Operational Hydrologic Remote Sensing Center (NOHRSC) [*Carroll et al.*, 2001]. First of all, the
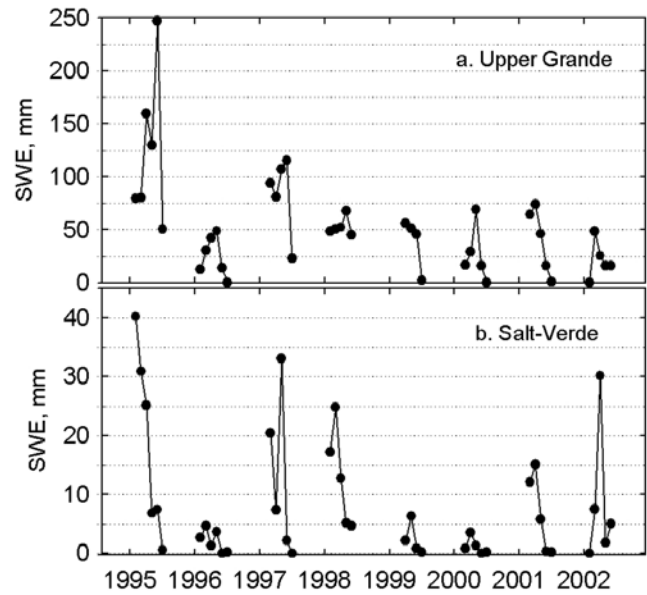

Figure 10. SWE amounts for (a) upper Grande and (b) Salt-Verde basins, based on blended satellite (SCA) and ground-based (SWE) products.

NOHRSC product is binary and our product provides an estimate of fraction SCA in each pixel. Second, even comparing the fraction of pixels in a basin with detectable snow there are important differences. In the upper Colorado the daily NOHRSC SCA estimates are as little as 15% of our SCA values during accumulation (January–March) and as much as 96% higher during ablation (April–June); on average the NOHRSC estimate is 5.5% higher (Figure 13a). Basin-scale differences between the fraction of pixels with detectable snow from NOHRSC versus the current mapping are less extreme for the lower Colorado, with NOHRSC overestimating by an average of 3.3% (data not shown). The NOHRSC overestimation of basin SCA during ablation
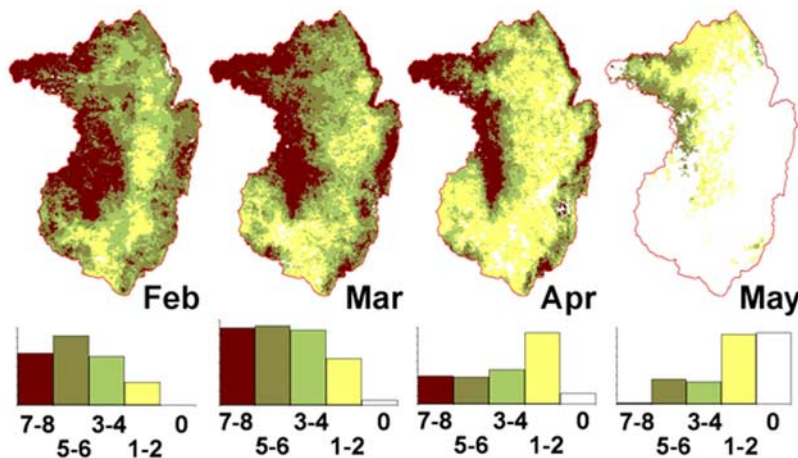

Figure 9. SCA persistence for upper Grande basin over the 1995–2002 period for months in which scenes were available for all 8 years, reported as number of years each pixel had detectable snow cover during that month. Note that January and June had data in fewer than 8 years. Heights of bars indicate relative magnitude of persistence across all pixels.
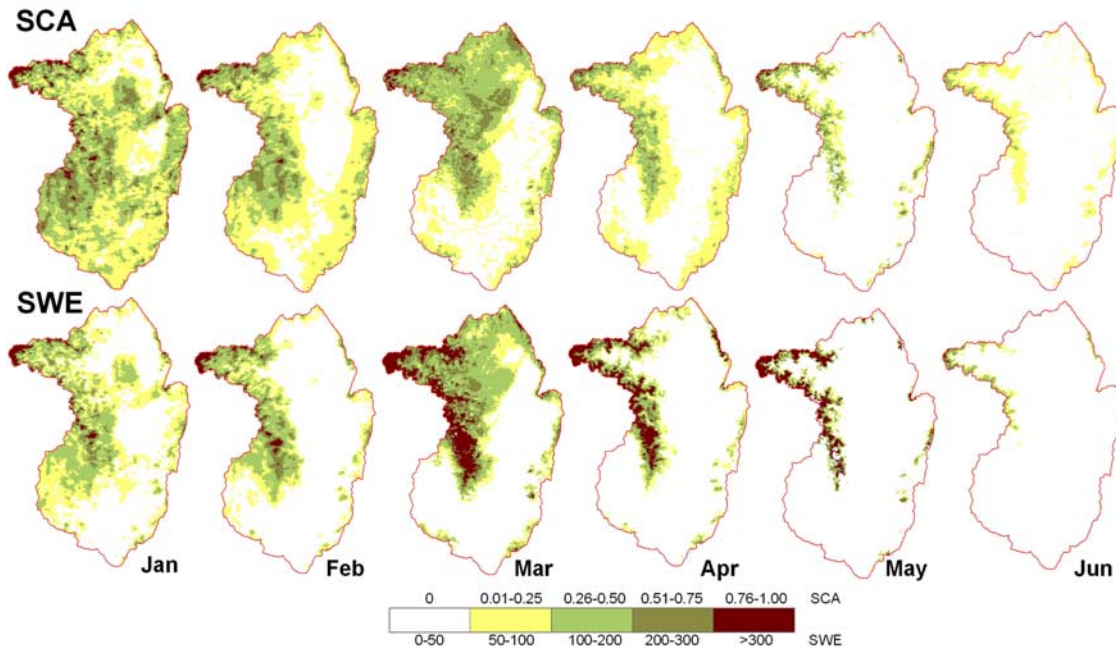
Figure 11. Upper Grande SCA and SWE for 1995, binned into four classes each.

occurs in part because in the binary classification a pixel with detectable snow cover is assigned a SCA of 100%. However, most pixels actually have a low-fraction SCA (Figure 4). For example, in the upper Colorado, basin average snow cover during the early part of the ablation season in a wet year, using the fractional SCA product, is 12–15% (Figure 5). However, 30–50% of the pixels may have detectable snow (Figure 4). Thus a binary classification significantly overestimates the snow cover amount.

[24] On average, NOHRSC classified 6% more pixels as cloud in the upper Colorado than did our approach and 3% more pixels in the lower Colorado (Figure 13b). Differences in individual scenes were much larger. The NOHRSC product relied on an automated cloud-masking algorithm, whereas our product is based on a custom, scene-by-scene masking of clouds. *Maurer et al.* [2003] compared the binary SCA product from NASA's MODIS to that from NOHRSC. MODIS classified 14% fewer pixels as cloud over topographically complex terrain, and classified 12% more pixels as SCA than did NOHRSC. However, it should be noted that in addition to using a different cloud-masking algorithm, MODIS has a different overpass time than does AVHRR. *Klein and Barnett* [2003] also found that for the
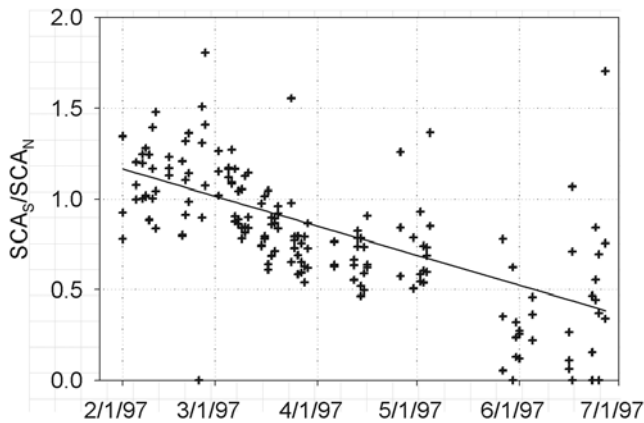

Figure 12. Ratio of SCA mapped on south facing slopes (SCA_S) to that on north facing slopes (SCA_N) for upper Grande, elevation bands 2900–3800 m.
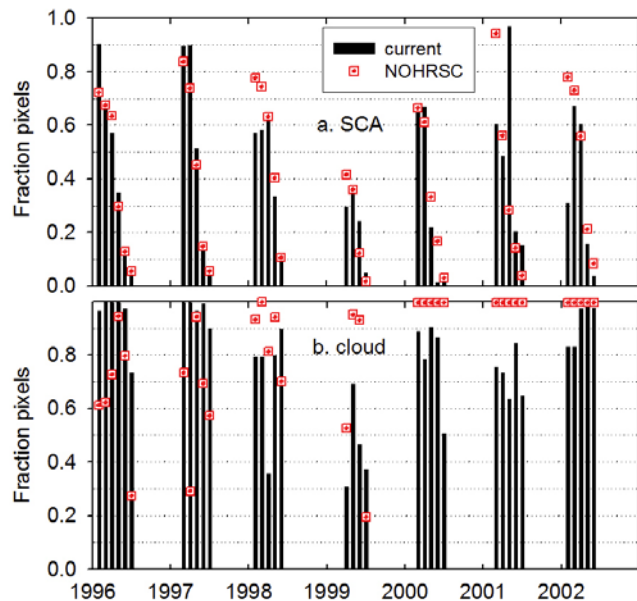

Figure 13. Fraction of pixels with (a) detectable SCA and (b) cloud for current products versus those from NOHRSC, for the same days and averaged over the same periods, for upper Colorado basin. NOHRSC data are not available for 1995.

2001 snow season, the MODIS binary product consistently gave a slightly higher proportion of the Rio Grande basin as snow covered than did the NOHRSC product.

[25] The higher frequency of clouds in 2002 is related to the real-time processing of the scenes, with many cloudy scenes being used in the analysis. Over the 8-year period, cloud cover was more frequent in the upper Colorado relative to the lower Colorado (Figure 2) and is correlated to snow cover trends. Clouds are most frequent along the high elevations of the basin boundaries, the same locations of persistent interannual and intra-annual snow cover.

[26] One unaccounted for bias in all SCA products is forest. We did not correct for canopy opening, and the satellite only "sees" snow between trees. The exception is right after a storm, when there is snow in the canopy [*Dressler et al.*, 2006]. Errors are particularly acute at high zenith angles, for which no corrections were made. High zenith angles result in larger pixel sizes and more masking of snow by canopy.

[27] Mapping snow products at resolutions no coarser than about 1 km^2 is desirable in order to capture the terrain heterogeneity that controls snow cover in mountains, especially considering that during much of the year snow primarily occurs in high-elevation areas that are a few km to tens of km wide. However, another source of error is georegistration and orthorectification. For the current product, errors of 1–2 km are visually observed.

6. Conclusions

[28] Areas with persistent snow cover are relatively reproducible from year to year, and correspond to higher elevations. Some snow accumulates on about 50% of the 1-km^2 pixels in the upper Colorado even during dry years. The average SCA for all pixels having detectable snow cover varied from about 20% in dry to 30% in wet years. However, snow cover depletion patterns varied significantly from year to year. SCA patterns clearly show the wet (1995–1998) and dry (1999–2002) years within the 8-year period for which we mapped snow cover.

[29] An immediate application for the fractional product is to provide snowpack information for evaluating hydrologic models of snowmelt runoff and other components of the water balance. While the current SCA and combined SCA-SWE product are a step toward improved spatial snow estimates, there are several areas for improvement, including: (1) using vegetation information to improve snow mapping in forested areas, (2) developing more representative ground-based measurements, and (3) using data with greater spectral resolution, e.g., MODIS, to improve discerning snow from other features. The current SCA products are available online (www.sahra.arizona.edu) and both products and raw data on CD by request.

References

Blöschl, G., R. Kirnbauer, and D. Gutknecht (1991), Distributed snowmelt simulations in an alpine catchment: 1. Model evaluation on the basis of snow cover patterns, *Water Resour. Res.*, 27(12), 3171–3179.

Carroll, T. R., D. W. Cline, G. Fall, A. Nilsson, L. Li, and A. Rost (2001), NOHRSC operations and simulation of snow cover properties for the coterminous U. S., paper presented at 69th Annual Meeting of the Western Snow Conference, AGU, Sun Valley, Idaho.

Daly, S. F., R. E. Davis, E. Ochs, and T. Pangburn (2000), An approach to spatially distributed snow modeling of the Sacramento and San Joaquin basins, California, *Hydrol. Processes*, 14, 3257–3271.

Davis, R. E., T. Pangburn, S. F. Daly, E. Ochs, J. P. Hardy, E. Bryant, R. Bolus, J. Laprevote, and P. Pugner (1999), Can satellite snow maps, ground measurements and modeling improve water management and control in the Kings River Basin, California?, paper presented at 67th Annual Meeting of the Western Snow Conference, AGU, S. Lake Tahoe, Calif.

Dozier, J. (1989), Spectral signature of alpine snow cover from the Landsat thematic mapper, *Remote Sens. Environ.*, 28, 9–22.

Dozier, J., S. R. Schneider, and D. F. McGinnis Jr. (1981), Effect of grain size and snowpack water equivalence on visible and near-infrared satellite observations of snow, *Water Resour. Res.*, 17(4), 1213–1221.

Dressler, K. A., G. Leavesley, R. C. Bales, and S. R. Fassnacht (2006), Evaluation of gridded snow water equivalent and satellite snow cover products for mountain basins in a hydrologic model, *Hydrol. Processes*, 20, 673–688.

Elder, K., and J. Dozier (1990), Improving methods for measurement and estimation of snow storage in an alpine watershed, in *Hydrology in Mountainous Regions I: Hydrological Measurements, the Water Cycle*, edited by H. Lang and A. Musy, *IAHS Publ.*, 193, 147–156.

Elder, K., J. Dozier, and J. Michaelsen (1991), Snow accumulation and distribution in an alpine watershed, *Water Resour. Res.*, 27(7), 1541–1552.

Fassnacht, S. R., K. A. Dressler, and R. C. Bales (2003), Snow water equivalent interpolation for the Colorado River Basin from snow telemetry (SNOTEL) data, *Water Resour. Res.*, 39(8), 1208, doi:10.1029/2002WR001512.

Foppa, N., S. Wunderle, A. Hauser, D. Oesch, and F. Kuchen (2004), Operational sub-pixel snow mapping over the Alps with NOAA AVHRR data, *Ann. Glaciol.*, 38, 245–252.

Gutzler, D. S., and J. W. Preston (1997), Evidence for a relationship between spring snow cover in North America and summer rainfall in New Mexico, *Geophys. Res. Lett.*, 24(17), 2207–2210.

Klein, A. G., and A. C. Barnett (2003), Validation of daily MODIS snow cover maps of the Upper Rio Grande River Basin for the 2000–2001 snow year, *Remote Sens. Environ.*, 86, 162–176.

Martinec, J., K. Seidel, U. Burkhart, and R. Baumann (1991), Areal modeling of snow water equivalent based on remote sensing techniques, in *Snow, Hydrology and Forests in High Alpine Areas*, edited by H. Bergmann et al., *IAHS Publ.*, 205, 121–129.

Maurer, E. P., J. D. Rhoads, R. O. Dubayah, and D. P. Lettenmaier (2003), Evaluation of the snow-covered area data product from MODIS, *Hydrol. Processes*, 17, 59–71.

Metsämäki, S., J. Vepsäläinen, J. Pulliainen, and Y. Sucksdorff (2002), Improved linear interpolation method for the estimation of snow-covered area from optical data, *Remote Sens. Environ.*, 82, 64–78.

Metsämäki, S. J., S. T. Anttila, H. J. Markus, and J. M. Vepsäläinen (2005), A feasible method for fractional snow cover mapping in boreal zone based on a reflectance model, *Remote Sens. Environ.*, 95, 77–95.

Phulpin, T., J. P. Jullien, and D. Lasselin (1989), AVHRR data processing to study the surface canopies in temperate regions—1st results of HAPEX-MOBILHY, *Int. J. Remote Sens.*, 10, 869–884.

Rango, A., and J. Martinec (1979), Application of a snowmelt-runoff model using Landsat data, *Nord. Hydrol.*, 10, 225–238.

Rosenthal, W., and J. Dozier (1996), Automated mapping of montane snow cover at subpixel resolution from the Landsat thematic mapper, *Water Resour. Res.*, 32(1), 115–130.

Saunders, R. W., and K. T. Kriebel (1988), An improved method for detecting clear sky and cloudy radiances from AVHRR data, *Int. J. Remote Sens.*, 9, 123–150.

Simpson, J. J., and R. H. Keller (1995), An improved fuzzy logic segmentation of sea ice, clouds, and ocean in remotely sensed Arctic imagery, *Remote Sens. Environ.*, 54, 290–312.

Simpson, J. J., J. R. Stitt, and M. Sienko (1998), Improved estimates of the areal extent of snow cover from AVHRR data, *J. Hydrol.*, 204, 1–23.

Vermote, E. F., D. Tanré, J. L. Deuzé, M. Herman, and J.-J. Morcrette (1997), Second simulation of the satellite signal in the solar spec-

trum, 6S: An overview, *IEEE Trans. Geosci. Remote Sens.*, *35*(3), 675–686.

Wen, S., and W. I. Rose (1994), Retrieval of sizes and total masses of particles in volcanic clouds using AVHRR bands 4 and 5, *J. Geophys. Res.*, *99*(D3), 5421–5432.

————————————

R. C. Bales, School of Engineering, University of California, P.O. Box 2039, Merced, CA 95344, USA. (rbales@eng.ucmerced.edu)

K. A. Dressler, Penn State Institutes of Energy and the Environment, Pennsylvania State University, 129 Land and Water Research Building, University Park, PA 16802, USA.

S. R. Fassnacht, Watershed Science Program, Colorado State University, Natural Resources Building Room 335, Fort Collins, CO 80523-1482, USA.

B. Imam, Department of Civil and Environmental Engineering, Henry Samueli School of Engineering, University of California, UCRP 250G, Irvine, CA 92697-2175, USA.

D. Lampkin, Department of Geography, Pennsylvania State University, Room 313 Walker Building, University Park, PA 16802, USA.